Research Article

Received: 9 July 2024 Revised: 17 April 2025 Published online in Wiley Online Library:

(wileyonlinelibrary.com) DOI 10.1002/jctb.7919

Effects of temperature on biofilm formation and resource recovery during anoxyphototrophic treatment of fuel-synthesis wastewater

Sultan Shaikh,[a*] Soumia Gasmi,[b] Adriaan Stephanus Luyt,[b] Gordon McKay[a] and Hamish Robert Mackey[a,c]

Abstract

BACKGROUND: Fuel-synthesis wastewater (FSW), a byproduct of the Fischer-Tropsch process, requiring efficient treatment and resource recovery strategies. This study aimed to optimize temperature conditions for purple non-sulfur bacteria (PNSB) biofilm formation and bioproduct recovery while simultaneously treating FSW. Experiments were conducted in biofilm photobioreactors operated at 30 °C, 35 °C, and 45_°C under illuminated anaerobic conditions. The study evaluated PNSB growth, wastewater treatment efficiency, and the yields of bioproducts, including polyhydroxybutyrate (PHB), single cell protein (SCP), lipids, carbohydrates and pigments.

RESULTS: No PNSB growth was observed at 45 °C, while the highest suspended growth occurred at 35 °C and biofilm growth at 30 °C. Biofilm formation significantly increased PHB accumulation (17%) compared to suspended growth (4.3%–7.4%), highlighting the efficiency of biofilm-based cultivation. Temperature had a minimal effect on PHB composition but influenced its crystallinity and morphology. The protein content remained consistent across conditions, while lipids increased with temperature.

CONCLUSION: Temperature selection between 30 °C and 35 °C significantly influences biofilm *versus* suspended biomass ratios and differentially affects bioproduct yields. Biofilm cultivation is preferable for maximizing PHB recovery, indicating potential for sustainable resource recovery and wastewater treatment strategies, particularly in tropical regions where external temperature regulation may be unnecessary.

Supporting information may be found in the online version of this article.

Keywords: climate; purple non-sulfur bacteria; gas to liquids (GTL) wastewater; circular economy; biofilm

INTRODUCTION

Fuel-synthesis wastewater (FSW) is a byproduct generated during the Fischer-Tropsch process, where natural gas is converted into liquid fuel. This process produces a substantial volume of wastewater, with the largest facility generating 45,000 m^3 per day.[1] Globally, FSW production is estimated at 32 million m^3 yr^{-1}, and this number is expected to rise with increasing oil prices.[2] FSW is characterized by high acidity and organic content, with a chemical oxygen demand (COD) of up to 32 g L^{-1}, consisting mainly of dissolved organic acids and alcohols.[3] Given its composition, FSW presents both an environmental challenge and an opportunity for resource recovery. In recent years, the concept of a circular economy has gained attention as an approach to minimize waste and maximize resource reuse, shifting away from the traditional linear production-consumption-waste model. The recovery of valuable resources from industrial wastewater aligns with this concept.[4] Among the various biotechnological strategies for wastewater treatment and resource recovery, microbial-based approaches offer a sustainable and cost-effective solution.[5,6]

* *Correspondence to: S Shaikh, Division of Sustainable Development, College of Science and Engineering, Hamad bin Khalifa University, Qatar Foundation, Doha, Qatar. E-mail: sultanshaikhmuet@gmail.com*

a *Division of Sustainable Development, College of Science and Engineering, Hamad bin Khalifa University, Qatar Foundation, Doha, Qatar*

b *Center for Advanced Materials (CAM), Qatar University, Doha, Qatar*

c *Department of Civil and Natural Resources Engineering, University of Canterbury, Christchurch, New Zealand*

Purple non-sulfur bacteria (PNSB) are facultative anaerobes capable of degrading pollutants while synthesizing valuable bioproducts such as polyhydroxybutyrate (PHB), single-cell protein, lipids, carbohydrates, carotenoids (Crts) and bacteriochlorophylls (BChls). These metabolites have applications in bioplastics, animal feed, biofuels and pharmaceuticals.[7,8] PNSB can be cultivated in both suspended and biofilm growth modes, with biofilm-based cultivation offering advantages such as higher biomass retention, increased stability and easier cell harvesting.[9]

Temperature plays a critical role in the metabolic activity, growth and resource recovery potential of PNSB. Studies have shown that certain thermotolerant strains of PNSB can survive and function at high temperatures. Charlton[10] investigated thermotolerant PNSB isolated from geothermal regions in New Zealand, highlighting their ability to grow optimally at around 40 °C, with maximum growth temperatures ranging from 43 °C to 47 °C. His study also identified thermotolerant and mildly thermophilic strains from thermal areas, suggesting that some PNSB species can thrive at elevated temperatures. Similarly, Hisada *et al.*[11] isolated phototrophic PNSB from hot spring microbial mats developing at 50 °C–65 °C in Japan and cultivated them under phototrophic conditions at 50 °C and 37 °C. Their study found that most PNSB isolates grew at temperatures up to 45 °C, with optimal growth at around 40 °C, indicating that hot springs provide a favorable ecological niche for PNSB adaptation to high temperatures. In addition to microbial isolation studies, temperature-dependent enzymatic and metabolic activity in PNSB has been studied in species such as *Rhodospirillum rubrum* and *Rhodobacter sphaeroides*. Kaftan *et al.*[12] found that photosynthetic electron transport in *Rhodospirillum rubrum* was active up to 41 °C but irreversibly inhibited above this threshold, with photochemistry functional until 60 °C. Similarly, Kaiser and Oelze[13] observed that ATPase and succinate cytochrome c oxidoreductase in *Rhodospirillum rubrum* and *Rhodopseudomonas sphaeroides* exhibited temperature-dependent discontinuities at 19 °C–20 °C, while NADH respiration remained continuous.

PNSB-based biopolymer production is also influenced by temperature. Lee *et al.*[14] optimized growth conditions for PHB production in *Rhodobacter sphaeroides*, identifying 30 °C as the most effective temperature for PHB accumulation, with a carbon-to-nitrogen ratio of 9:1 or higher promoting maximum yields. Likewise, Lo *et al.*[15] optimized *Rhodopseudomonas palustris* fermentation using low-cost media and identified an optimal temperature of 37.9 °C for biomass production.

While previous studies have examined PNSB thermotolerance, enzymatic activity and biopolymer production at different temperatures, systematic investigations of temperature effects on biofilm formation remain limited. Most studies have focused on suspended growth, leaving a knowledge gap regarding how temperature influences microbial adhesion, extracellular polymeric substance production and biofilm stability. Moreover, a notable study by Hülsen *et al.*[16] examined temperature variations (6 °C–55 °C) in naturally illuminated photobioreactors, reporting no significant effect on purple phototrophic bacteria performance. However, this study was conducted in outdoor conditions under diurnal and daily variations in temperature, lacking controlled laboratory conditions to systematically evaluate temperature effects.

The study reported here aimed to systematically evaluate the effect of temperature (30 °C, 35 °C and 45 °C) on PNSB biofilm formation and metabolic activity under nitrogen-limited conditions, addressing gaps in previous research. Temperatures of 30 °C and 35 °C were chosen as they fall within the optimal growth range for PNSB, supporting active metabolism and resource recovery, while 45 °C was included to assess the upper thermal tolerance and its impact on microbial survival. Unlike prior studies, this research examined the competitive dynamics between biofilm and suspended growth under controlled laboratory conditions, allowing for a more precise understanding of temperature-driven microbial selection and resource accumulation mechanisms.

MATERIALS AND METHODS

Biofilm photobioreactor and growth conditions

Six laboratory-scale biofilm photobioreactors (BPBRs) were utilized. Each BPBR was constructed from a wide-mouthed glass bottle with a total volume of 2 L and a working volume of 1.7 L.

Three different temperature conditions were examined, 30 °C, 35 °C and 45 °C, with each run as biological duplicates simultaneously. The experiments were conducted under illuminated anaerobic conditions, with a constant average light incidence of 100 W m^{-2}. The light was provided by 30 W flood white light kept at 15 cm from the wall of the BPBR. The initial pH of the BPBRs was set to 7.7 and was not controlled through the study. To ensure adequate mixing and temperature control, each BPBR was agitated at 100 rpm using a magnetic stirrer with hot plate. The temperature of the liquid was monitored before sample collection using a thermometer. The experiment ran for 15 days.

To support biofilm formation, agricultural shade cloth sheets (30.48 cm × 15.24 cm) with mesh opening size of approximately 600 μm–800 μm were placed within the BPBRs. The agricultural shade cloth was rolled into a tube so that it sat around the internal walls of bioreactor but was able to rotate under mixing. The agricultural shade cloth was chosen as the biofilm support strata due to a structure that allows both protected areas for biofilm colonization and good light penetration. Additionally, it has proved effective for PNSB biofilm formation in our previous studies.[9,17]

A schematic of the experimental setup is provided in Fig. 1. To ensure anaerobic conditions, all BPBRs were flushed with nitrogen for 2 min prior to the start of the experiments. At the end of the experiment, PHB, SCP, lipids carbohydrates, Crts and BChls were quantified from the biofilm and suspended biomass. PHB was further characterized using a range of techniques described subsequently.

PNSB growth media

For this experiment, a mixed culture enriched with PNSB that had previously been grown on FSW with nitrogen-deficient media was used as an inoculum. FSW with nitrogen-deficient media was also used as growth media in this experiment since nitrogen-deficient media enhance the formation of PNSB biofilm.[9,17] The characteristics of FSW used in this experiment are presented in Table S1 in the supporting information. To the FSW the following were added: KH_2PO_4 (3.03 g L^{-1}), $NaHCO_3$ (4.29 g L^{-1}), ATCC trace minerals solution (10 mL L^{-1}) and ATCC vitamins solution (10 mL L^{-1}). The composition of the ATCC trace minerals solution and vitamins solution was the same as in our previous study.[9]

Biomass determination and quantification

To measure the growth of biomass in suspension, absorbance at 420 nm was determined using a UV-3600 Plus spectrophotometer (Shimadzu, Japan). At the end of the experiment, the biomass

Journal of Chemical Technology and Biotechnology published by John Wiley & Sons Ltd on behalf of Society of Chemical Industry (SCI).

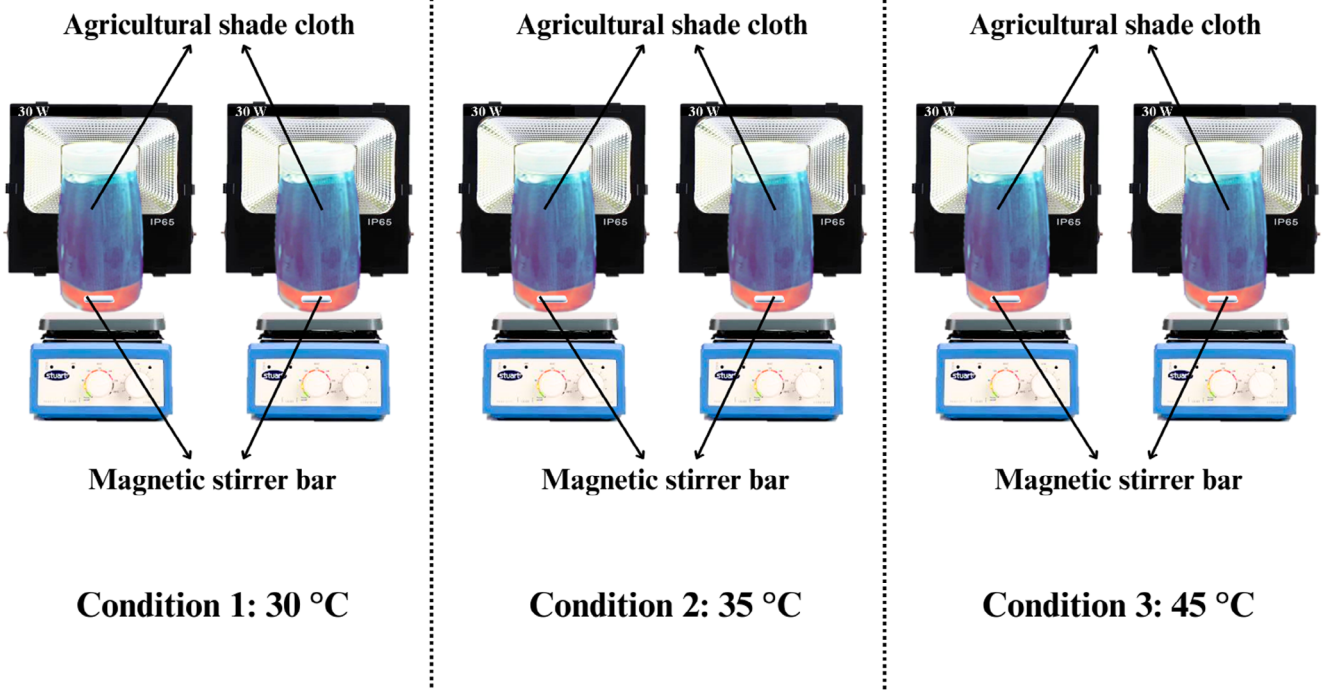

Figure 1. Experimental setup used in the study.

growth was further quantified using standard volatile suspended solids (VSS) and total suspended solids (TSS) methods.[18] The biomass attached to the agricultural shade cloth was initially dislodged using a predetermined volume of distilled water. To enable a significant comparison of growth in suspension *versus* biofilm formation, measurements of TSS and VSS were quantified by mass instead of concentration.

Water quality analysis

In this study, pH, oxidation-reduction potential (ORP), COD, total carbon (TC), inorganic carbon (IC), total organic carbon (TOC) by difference and total nitrogen (TN) were measured every third day. The pH and ORP were measured using a multi-parameter meter (Orion Star, Thermo Scientific, USA) by opening the bottle and measuring immediately. To analyze COD, TOC, TC, IC and TN, samples of the effluent wastewater were collected, centrifuged and filtered through a 0.2 μm Nalgene syringe filter to obtain the supernatant. COD of the supernatant was determined on the same day of sample collection, while the other parameters were determined within 48 h. The samples were stored at 4 °C until analysis. COD was measured using the USEPA Reactor Digestion Method 8000[19] with high-range COD vials (Hach, USA). TOC, TC and IC were measured using a TOC-L Analyzer (TOC-L CSH, Shimadzu, Japan). TN was measured using a TNM-L Analyzer (TNM-ROHS, Shimadzu, Japan).

PHB extraction, quantification and characterization

PHB is the most prevalent polyhydroxyalkanoate type, both for bacteria in general and for PNSB.[20] PHB was extracted and quantified using sodium hypochlorite digestion and UV spectrophotometry, as reported in our previous study.[17] For PHB characterization, differential scanning calorimetry (DSC) was used to determine the thermal properties of the extracted PHB, such as the melting point, crystallization behavior and enthalpy of transitions. DSC analysis was performed using a differential scanning calorimeter (DSC8500, PerkinElmer, USA) under a nitrogen atmosphere. The analysis was performed using 3 mg–5 mg samples, heating them from −60 °C to 200 °C at 10 °C min^{-1}. The samples were then cooled to −60 °C and re-heated to 200 °C, both at the same rate.

Thermogravimetric analysis (TGA) was used to evaluate the thermal stability of the PHB polymer. This technique involves monitoring the changes in weight of a sample as its temperature is raised, providing valuable information about the material's ability to maintain its physical and chemical properties under elevated temperatures.[21] TGA was performed using a TGA-4000 (PerkinElmer, USA). A sample of 3 mg–5 mg was heated from 30 °C to 900 °C at a heating rate of 10 °C min^{-1} in a nitrogen atmosphere.

Fourier transform infrared (FTIR) spectroscopy was used to identify functional groups in the extracted PHB through their absorption of infrared radiation to confirm the material composition. An FTIR spectrometer (Frontier Spectrum 400, PerkinElmer, USA) connected to a MIRACLE ATR detector with a ZnSe crystal was used to obtain FTIR spectra at room temperature. A total of 32 scans in the range 500 cm^{-1}–4000 cm^{-1} were done on each sample at a resolution of 4 cm^{-1}.

X-ray diffraction (XRD) was used to determine the crystal structure of the extracted PHB material using an X'Pert PRO X-ray diffractometer (Malvern Panalytical, UK) with Co Kα (1.789 Å) radiation at a voltage of 45 kV and a current of 40 mA. Samples were scanned under a diffraction angle of 2θ ranging from 5° to 90°.

Journal of Chemical Technology and Biotechnology published by John Wiley & Sons Ltd on behalf of Society of Chemical Industry (SCI).

Protein extraction and quantification

Cellular protein was determined by the Lowry protein assay method using bovine serum albumin as the reference protein.[22] For the Lowry protein assay, the alkaline extraction technique described by Perovic *et al.*[23] was used to extract the cellular protein from suspended and biofilm samples with a few minor modifications, as described in Shaikh *et al.*[9]

Lipid extraction and quantification

The total lipid content of the PNSB biomass obtained from both suspended and biofilm growth was extracted and quantified using a modified Bligh-Dyer method.[24] A sample of freeze-dried PNSB biomass (30 mg) was homogenized with 5 mL of chloroform in a 40 mL glass tube. Subsequently, 10 mL of methanol was added, and the mixture was vigorously agitated. An additional 5 mL of chloroform was added and mixed again. The mixture was then allowed to phase separate by the addition of 5 mL of distilled water and incubated overnight. The lower phase, containing the lipids, was collected using a glass Pasteur pipette and transferred to a pre-weighed glass vial. The vial was then placed in an oven at 100 °C for complete evaporation and drying. The weight of the dried vial was measured, and the lipid content was calculated as a percentage using Eqn (1):

$$\text{Lipid content}\,(\%) = \frac{(w_2 - w_1) \times V_o}{W \times V_e} \quad (1)$$

where w_1 = weight of empty glass vial (mg), w_2 = weight of glass vial + dried lipids (mg), V_o = volume of organic phase (mL), W = weight of PNSB biomass used initially (mg), and V_e = evaporated volume (mL).

Carbohydrate extraction and quantification

The carbohydrate content of PNSB biomass was extracted and quantified using a modified anthrone method and glucose as standard, as reported by Morris.[25] A sample of PNSB freeze-dried biomass (20 mg) was homogenized with 5 mL of 2.5 N HCl in a 40 mL glass tube, which was then heated in a water bath at 90° C for 3 h. After cooling, the samples were transferred to 50 mL falcon tubes and 45 mL of distilled water was added to each sample, which was then centrifuged at 5000 × *g* for 20 min in a centrifuge (Sorvall LYNX 6000, Thermo Scientific, USA). An amount of 1 mL of the supernatant was collected in 40 mL glass tubes to which 5 mL of anthrone reagent was added. The mixture was then heated in a water bath at 90 °C for 20 min. After cooling, the absorbance was measured at 620 nm using a UV-3600 Plus spectrophotometer (Shimadzu, Japan). The carbohydrate content was calculated as a percentage using Eqn (2):

$$\text{Carbohydrate content}\,(\%) = \frac{C \times V}{W} \times 100 \quad (2)$$

where C = concentration of carbohydrates obtained from standard curve (mg L^{-1}), V = total volume of deionized water + HCl (L), and W = weight of PNSB biomass used initially (mg).

Photopigments extraction and quantification

The concentrations of Crts and BChls in both biofilm and suspended biomass were measured at the end of the experiment. Crts were extracted using acetone, while BChls were extracted using a 7:2 (v/v) acetone-to-methanol ratio, following previously reported method[26] with modification. The detailed extraction and analysis procedures have been reported in a previous study.[17]

Statistical analysis

Data analysis was carried out using a completely randomized design and analysis of variance (ANOVA) in Statistix 10 software. After the ANOVA, further comparisons between the groups were made using the Bonferroni correction method, with a significance level of 5%.

RESULTS AND DISCUSSION

PNSB biomass and growth

Final biomass quantities from suspended and biofilm growth are shown in Fig. 2(a) for the two BPBRs having incubation temperatures of 30 °C and 35 °C. The BPBR at 45 °C showed no growth for either suspended or biofilm growth, consistent with that reported by Branakarl *et al.*,[27] who reported that PNSB failed to grow under anaerobic conditions at 45 °C unless co-cultured with an aerobic bacterium. The suspended growth biomass quantities obtained from 30 °C and 35 °C conditions were 1020 ± 240 mg and 1615 ± 361 mg, respectively. The mass of biofilm was less, with 775 ± 132 mg and 589 ± 44 mg obtained from the 30 °C and 35 °C BPBRs, respectively. The biomass obtained in both conditions and growth modes were not statistically significantly different from each other ($P > 0.05$). A higher biofilm growth at 30 °C was also identifiable from visual inspection of the agricultural shade cloth (Fig. 2(b)–(d)). This is likely due to optimal growth conditions for PNSB at this temperature. Less biofilm formation was observed in the 35 °C condition, with higher VSS in suspended growth. Absorbance measurements of suspended growth were in line with VSS measurements, confirming greatest growth at 35 °C and negligible growth at 45 °C (Fig. 2(e)). However, differences in absorbance were small. A similar study by Sepúlveda-Muñoz *et al.*[28] investigated PNSB growth at two temperatures, 13 °C and 30 °C, using piggery wastewater as the substrate. They reported suspended biomass production of 575 ± 50 mg at 13 °C and 595 ± 40 mg at 30 °C. Compared to our study, their biomass at 30 °C (595 mg) was significantly lower than our 30 °C result (1020 mg) and 35 °C result (1615 mg). The lower biomass production in their study may be attributed to differences in reactor conditions, such as reactor size (0.5 L *versus* larger BPBR in this study), light intensity and wastewater composition. Piggery wastewater contains different organic and nutrient profiles compared to FSW, which may influence microbial metabolism and growth efficiency. Additionally, differences in inoculum adaptation and operational settings could further explain the variations in biomass accumulation. However, their study did not specifically investigate the effect of temperature on biofilm formation but focused on suspended biomass yields under different temperature conditions. Our study addresses this gap by evaluating the impact of temperature on both suspended and biofilm growth, providing new insights into biofilm-based resource recovery systems.

Similarly, Lo *et al.*[15] reported higher biomass production of *Rhodopseudomonas palustris* PS3 at 37 °C, reaching 2180 mg within 24 h of fermentation. The significantly higher yield compared to our study can be attributed to the use of a pure strain, an optimized growth medium containing molasses and corn steep liquor and controlled fermentation conditions. In contrast, our study utilized a mixed microbial culture enriched with PNSB, did not supplement nitrogen and used FSW as the substrate, which may

Journal of Chemical Technology and Biotechnology published by John Wiley & Sons Ltd on behalf of Society of Chemical Industry (SCI).

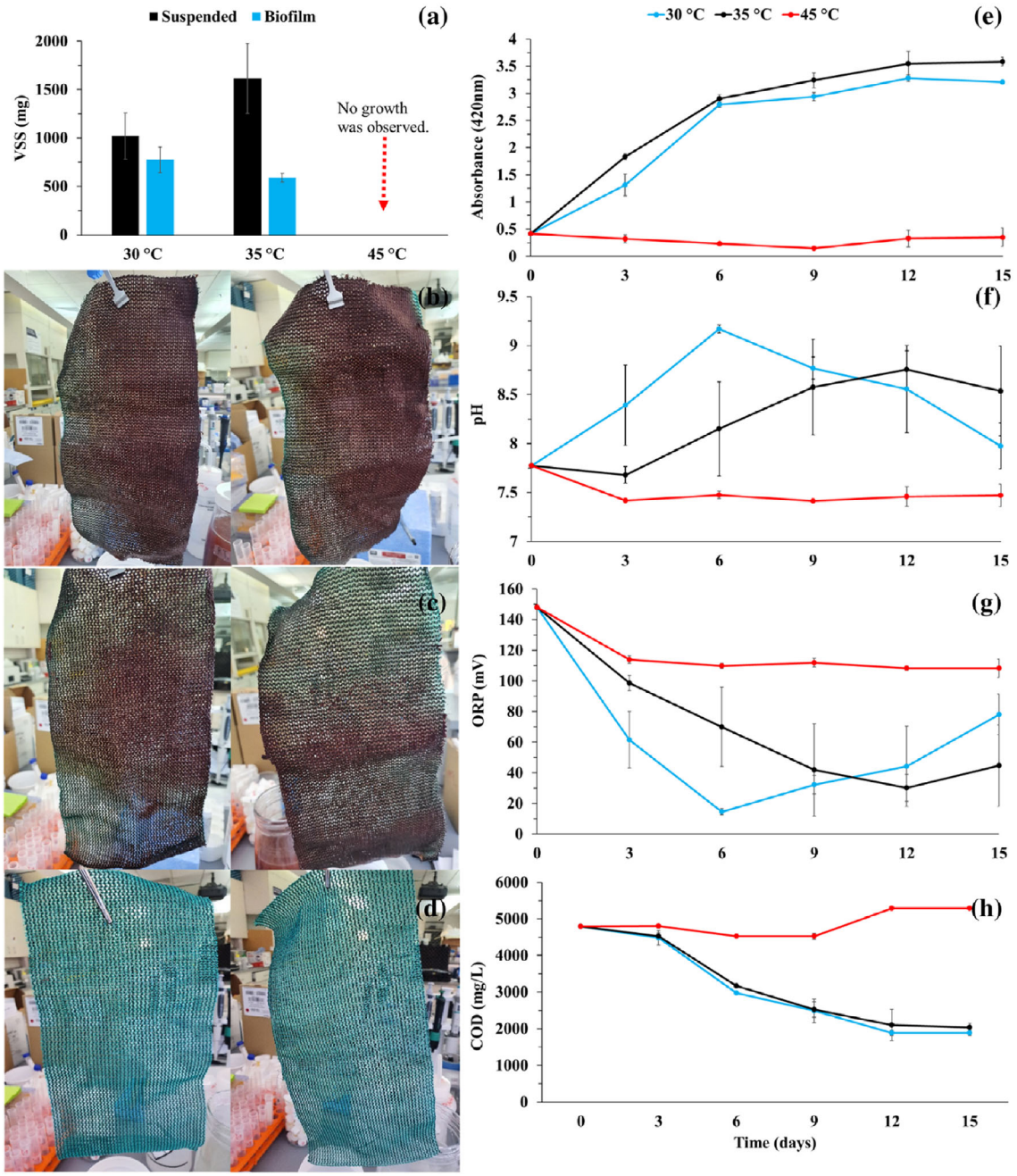

Figure 2. (a) Biomass production in suspended and biofilm growth. Biofilm formation in BPBRs operated at (b) 30 °C, (c) 35 °C and (d) 45 °C. Profiles of (e) absorbance, (f) pH, (g) ORP and (h) COD from all three BPBRs during the study.

have resulted in lower biomass accumulation. Hülsen *et al.*[16] undertook an outdoor study where temperatures varied naturally between 6 °C and 55 °C. They reported that temperature did not have a significant effect on biomass production in their mixed purple phototrophic system. However, their study focused on piggery and chicken processing wastewater treatment which is considerably different in composition; and was subjected to natural light cycles. These comparisons highlight that biomass production is strongly influenced by multiple factors, including microbial culture type (pure *versus* mixed), nitrogen availability, reactor conditions and wastewater composition. Our study, therefore, provides new insights into temperature-dependent biofilm formation and biomass accumulation, addressing the knowledge gap in biofilm-based PNSB wastewater treatment systems.

Changes in pH and ORP

Figure 2(f) illustrates the pH profile of the three different temperature conditions. The pH of the 30 °C condition showed a steady and substantial increase, reaching a peak of 9.17 ± 0.04 on day 6 before gradually decreasing. In contrast, the pH of the 35 °C condition remained stable until day 3 before gradually increasing, reaching a maximum of 8.75 ± 0.19 on day 12, then slightly decreasing. For the 45 °C condition, the pH decreased slightly at day 3 and remained constant for the duration of the test. The observed increase in pH for the lower-temperature conditions may be

Journal of Chemical Technology and Biotechnology published by John Wiley & Sons Ltd on behalf of Society of Chemical Industry (SCI).

indicative of elevated metabolic activity, potentially leading to enhanced CO_2 production. The pH increase observed at 30 °C and 35 °C is likely due to the photoheterotrophic metabolism of PNSB, which involves the oxidation of VFAs to generate ATP and reducing power for carbon fixation via the Calvin cycle. This process can lead to the production of basic metabolic intermediates such as bicarbonate and hydroxy ions, which can increase the pH.[29]

The initial ORP value for all temperature conditions was 148 ± 0.35 mV. These values are in the anoxic/micro-aerobic zone and suggest some oxygen seepage into the system, though the values are also likely to be higher than actual due to the open-vessel measurement. Figure 2(g) shows the ORP profile for the three temperature conditions. An inverse relationship was observed between ORP and pH. The ORP for the 30 °C condition showed a decreasing trend in the initial days, reaching a minimum of 14.65 ± 2.0 mV on day 6 before increasing again. The ORP for the 35 °C condition decreased to a minimum value of 30.2 ± 8.9 mV on day 12, then slightly increased. On the other hand, the ORP for the 45 °C condition decreased at day 3 and remained relatively constant at around 109 ± 1.69 mV for the duration of the test. These ORP measurements are consistent with values reported as favorable for PNSB dominance in wastewater systems.[30]

Carbon utilization

COD results

The COD profiles of all three temperature conditions are shown in Fig. 2(h). The COD reduction was initially slow for all reactors up to day 3. Beyond this, degradation began to occur in the 30 °C and 35 °C conditions and continued up to day 12. For the 45 °C condition a slight reduction in COD occurred, followed by an increase, possibly through biomass lysis. After day 12 up to day 15, COD in all conditions remained constant. Suspended biomass growth (absorbance measurements) was inversely correlated ($r > -0.90$) with COD reduction for 30 °C and 35 °C. This was not the case for the 45 °C condition, which had a moderate positive correlation ($r = 0.58$). The COD removal at 30 °C, 35 °C and 45 °C was 2900 ± 70.7 mg L^{-1}, 2750 ± 113 mg L^{-1} and − 495 ± 21.2 mg L^{-1}, respectively. The corresponding COD removal efficiency in all conditions obtained was 60.5 ± 1.47%, 57.4 ± 2.36% and −10.3 ± 0.44%. Removals at 30 °C and 35 °C were statistically similar ($P = 0.451$).

TOC and IC

The TOC reduction under conditions of 30 °C, 35 °C and 45 °C was 64.8 ± 0.3%, 62.7 ± 2.1% and 6.5 ± 2.2%, respectively, over the test duration (Fig. 3(a)). The lower TOC reduction at 45 °C suggests reduced PNSB activity, consistent with other parameter measurements. The TOC reduction at 30 °C was slightly higher than at 35 °C, as observed for COD removal, but the difference was not statistically significant ($P = 0.285$).

The IC content increased in all three conditions over time, but the 45 °C condition exhibited only a minor increase (Fig. 3(b)). A 150 mg L^{-1}–163 mg L^{-1} increase in IC was observed under the 30 °C and 35 °C conditions. This rise is attributed to the degradation of organic acids by PNSB, leading to CO_2 production. Under nitrogen-deficient conditions, this process is coupled with hydrogen (H_2) production, where the oxidation of organic acids generates excess electrons utilized for H_2 evolution, concurrently producing CO_2 and contributing to the observed IC increase.[31]

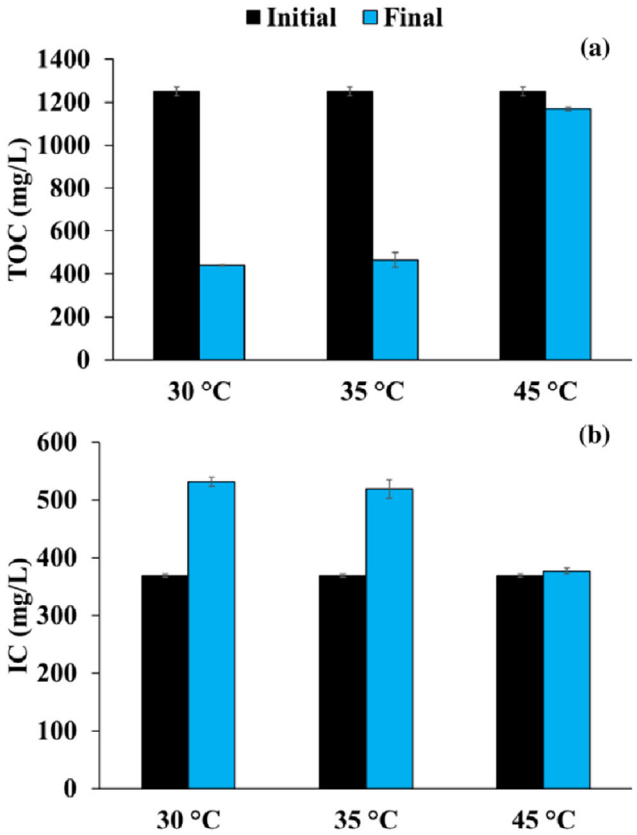

Figure 3. (a) TOC and (b) IC at initial and final days in all BPBRs.

Biomass yield

The biomass yield at 30 °C and 35 °C conditions was 0.36 ± 0.08 g-VSS (g-COD)$^{-1}$ and 0.47 ± 0.07 g-VSS (g-COD)$^{-1}$, respectively. These yields were not statistically different from each other ($P > 0.05$). The biomass yields observed in this study are consistent with those reported in other PNSB-enriched mixed culture studies using different types of wastewaters. These studies have reported yields ranging from 0.14 g-VSS (g-COD)$^{-1}$ to 0.66 g-VSS (g-COD)$^{-1}$,[32-36] which are lower than the optimal yields of around 0.68 g-VSS (g-COD)$^{-1}$, but higher than expected for anaerobic heterotrophs, supporting the active role of PNSB in the organic conversion process.

Resource recovery

Polyhydroxybutyrate

Temperature (30 °C and 35 °C) did not have a significant effect on PHB content in the biomass for either form of biomass ($P = 1.00$ for both). Insufficient biomass growth at 45 °C meant this condition could not be assessed for PHB or other bioproducts. However, biofilm showed at least 10% higher PHB content than the suspended growth in both temperature conditions ($P < 0.05$). In the suspended growth at 30 °C, the PHB content was found to be 7.4 ± 3.2%. However, in biofilm growth at 30 °C, the PHB content increased to 17.7 ± 1.8%. When the bacteria were grown at 35 °C, the PHB content in suspended growth decreased to 4.3 ± 3.0% (Table 1). However, in biofilm growth, the PHB content remained similar at 17.8 ± 4.0%. The total PHB production (suspended + biofilm) at 30 °C and 35 °C conditions was 421 ± 38 mg and 341 ± 153 mg with PHB yield

Journal of Chemical Technology and Biotechnology published by John Wiley & Sons Ltd on behalf of Society of Chemical Industry (SCI).

Table 1. Resource recovery from suspended and biofilm growth of different temperature conditions

	30 °C		35 °C	
Bioproduct	Suspended	Biofilm	Suspended	Biofilm
PHB (%)	7.4 ± 3.2	17.7 ± 1.8	4.3 ± 3.0	17.8 ± 4.0
Protein (Lowry) (%)	44.3 ± 1.4	40.1 ± 0.7	43.5 ± 0.2	40.7 ± 0.5
Lipids (%)	16 ± 0.1	20 ± 0.2	24 ± 0.1	22 ± 2.8
Carbohydrates (%)	8.0 ± 2.0	5.7 ± 2.4	6.3 ± 1.9	7.2 ± 1.2
Crts (%)	$(2.1 \pm 0.0) \times 10^{-4}$	$(2.1 \pm 0.0) \times 10^{-4}$	$(1.6 \pm 0.0) \times 10^{-4}$	$(1.7 \pm 0.0) \times 10^{-4}$
BChls (%)	$(1.2 \pm 0.0) \times 10^{-4}$	$(1.1 \pm 0.0) \times 10^{-5}$	$(6.9 \pm 0.0) \times 10^{-5}$	$(1.9 \pm 0.0) \times 10^{-5}$

of 85 ± 7.7 mg-PHB (g-COD)$^{-1}$ and 73 ± 32 mg-PHB (g-COD)$^{-1}$, respectively.

The greater accumulation of PHB in biofilm can be explained by light effects, given light intensity is a strong driver of PHB accumulation in PNSB.[37] As the agricultural shade cloth was closer to the wall of the BPBR it receives greater light exposure and causes shading to the cells present in the suspended growth mode. The diffusion restrictions in biofilms may also contribute to this effect, as Padovani *et al.*[38] proposed that the competition between PHB synthesis and H_2 production for reducing equivalents in biofilms may result in higher H_2 partial pressures and increased PHB synthesis. However, more research is needed to fully understand the mechanisms behind the observed PHB production in biofilm growth.

Comparing the differences in PHB for the suspended biomass under the two temperature conditions, various studies reported similar findings. For instance, Lee *et al.*[14] in their study tested *Rhodobacter sphaeroides* for PHB content under dark-aerobic conditions with different temperature conditions of 20 °C, 25 °C, 30 °C, 35 °C and 40 °C. They found 30 °C as the optima temperature condition for *Rhodobacter sphaeroides* to accumulate high cell densities of PHB, noting that temperatures above or below 30 °C significantly hindered growth and PHB synthesis. Similar results have also been reported for non-phototrophic bacteria; for instance, Asad-Ur-Rehman *et al.*[39] found that *Bacillus* sp. had a maximum PHB content of 53% at 30 °C, which decreased to 47% at 37 °C. This does not, however, explain why suspended growth responded to temperature while biofilm PHB content was constant. The observed differences are more likely caused by the slightly higher suspended growth in the 35 °C condition. This leads to increased shading in suspension, which may reduce PHB synthesis.

Single-cell protein

The protein content from suspended and biofilm growth at 30 °C and 35 °C was in the range of 40%–45% (Table 1). Suspended growth showed a slightly higher protein content (43.5%–44.3%) than the biofilm biomass (40.1%–40.7%). However, no significant difference was observed between the suspended growths ($P = 1.00$) of both conditions as compared to their respective biofilm growths. Likewise, statistically no significant difference was observed between the protein content of suspended growths ($P = 0.053$) as well as biofilm growths ($P = 0.197$) of both temperature conditions. The lower protein content is most likely linked to the higher PHB content observed in the biofilm. However, it may also be linked to the lower growth rates and activity resulting from mass transfer limitations. The findings of this experiment are similar to previous experiment results with same growth media (FSW and nitrogen deficient) where higher protein content of 43.9% was obtained in suspended growth as compared to biofilm growth with protein content of 42.6%. The total protein and protein productivities produced under both temperature and growth conditions ranges between 239 mg and 646 mg and between 16 mg-PN day^{-1}and 43 mg-PN day^{-1}, respectively. The large differences are based on biomass growth differences between biofilm and suspended growth.

Lipids and carbohydrates

The lipid content in the suspended and biofilm growth at 30 °C and 35 °C was obtained in the range of 16%–24% as presented in Table 1. It is observed that the highest lipid production was obtained at 35 °C suspended growth with 24 ± 0.1% and the lowest was from 30 °C suspended growth which was 16 ± 0.1%. It should be noted that the study found that the difference of lipid production from suspended growth of both conditions is significant ($P = 0.029$). However, no significant difference ($P = 1.00$) was observed between the biofilm growths of both conditions. The results suggest that higher temperature leads to increased lipid content in suspended growth. The observation of higher lipid production at 35 °C compared to 30 °C could be due to the increased metabolic activity of the microorganisms and the effect of temperature on enzyme activity. Higher temperatures can increase the activity of enzymes involved in lipid synthesis and could also alter the fluidity and permeability of cell membranes, making them more conducive to lipid synthesis.[40,41] Additionally, the higher temperature could create conditions that favor the accumulation of lipids as a way for the microorganisms to store excess carbon and energy.

Similar to lipids, temperature can have a significant effect on the production of carbohydrates by microorganisms. However, the specific effect of temperature on carbohydrate production can vary depending on the type of microorganism and the growth conditions.[42] In this study, the carbohydrate production under both conditions and growths was similar ($P > 0.05$) with a carbohydrate cell content range of 5%–8% (Table 1).

Photopigments

The Crt content was almost identical ($P = 1.00$) between suspended and biofilm growths for both temperature conditions. Likewise, the BChl content was similar between the suspended growth ($P = 0.257$) and biofilm growth ($P = 1.00$) of both temperature conditions. However, the Crts and BChls in suspended and biofilm growths of both temperature conditions have different values (Table 1).

Journal of Chemical Technology and Biotechnology published by John Wiley & Sons Ltd on behalf of Society of Chemical Industry (SCI).

The higher Crt content in the suspended and biofilm growth of 30 °C condition and higher BChls from suspended growth at 30 °C and higher BChls from biofilm growth at 35 °C could be due to the fact that PNSB mixed culture used in this study has different metabolic capabilities at different temperatures, leading to the observed differences in Crt and BChl content. Additionally, the physiology of the mixed culture at different temperatures might be different which might lead to different Crt and BChl content. The Crt and BChl contents obtained from this study (1.6 μg g^{-1}–2.1 μg g^{-1}) are lower than those reported in the literature from both PNSB pure (276 μg g^{-1}–10,750 μg g^{-1}) and mixed culture (4.3 μg g^{-1}–28.2 μg g^{-1}).[43–46] The findings of this study suggest that pursuing pigments may not be worthwhile. However, further optimization of pigment production may be possible.

PHB characterization

DSC

The DSC analysis results demonstrated that all PHB samples exhibited a two-step heating process at first heating with two peaks observed in the heating range of 150 °C–165 °C (Fig. 4). One possible reason for a double peak is the presence of impurities in the samples. These impurities can alter the thermal behavior of the material, leading to the appearance of multiple peaks. Alternative explanations include the presence of a copolymer, where each polymer may have a different melting temperature; or the crystalline structure of the material may be complex, resulting in multiple melting or recrystallization events. For PHB produced at 30 °C, both suspended and biofilm growth displayed almost similar peaks between 160 °C and 165 °C. In contrast, for PHB produced by biomass grown at 35 °C, peak magnitudes varied greatly between both samples. In terms of the cooling peaks, all samples exhibited a shallow peak in the temperature range of 50 °C–60 °C except for the 30 °C suspended growth sample, while the 35 °C biofilm sample showed a second peak at 90 °C. The dips correspond to the phase transitions of the PHB. During second heating, all samples showed more restrained peak separation, where one peak had become dominant. This indicates that PHB has undergone a partial melting or recrystallization during the first heating. This restrained double peak suggests that PHB has a high degree of crystallinity and a well-defined crystal structure. The presence of the restrained double peak can provide information about the quality and stability of the crystalline structure and the degree of thermal reversibility of PHB. Compared to the study by Mohd Zahari *et al.*,[47] where PHB produced from oil palm frond juice exhibited a melting temperature (T_m) of 162.2 °C, the PHB in our study showed a similar thermal range, reinforcing the notion that different carbon sources lead to only slight variations in thermal behavior. Additionally, the PHB produced from fructose in the Zahari *et al.* study exhibited a higher T_m of 177 °C, indicating that the type of substrate significantly influences the crystallization and thermal stability of PHB. The lower melting temperature observed in our samples may be attributed to differences in molecular weight, as previously suggested in the literature.

In summary, DSC analysis revealed that the PHB produced from suspended and biofilm growth at different temperatures exhibited distinct thermal properties with a number of peaks that look similar in most of the samples. However, the 30 °C suspended sample lacked a glass transition peak and a crystallization peak during cooling while the biofilm sample of 35 °C exhibited a double crystallization peak during cooling. These findings align with those reported by Mohd Zahari *et al.*,[47] where variations in crystallization behavior were observed depending on microbial growth conditions and carbon source utilization. Such variations highlight the influence of bioprocess parameters on the structural properties of PHB.

TGA

Figure 5 illustrates the TGA of PHB samples obtained from suspended and biofilm growth at 30 °C and 35 °C. The TGA results indicate that the maximum thermal degradation of all samples occurred in the range of 225 °C–249 °C, which is consistent with previous reports that describe the primary degradation of PHB occurring between 250 °C and 320 °C.[48]

The maximum thermal degradation of suspended and biofilm samples obtained at 30 °C is similar, whereas the maximum thermal degradation of both samples obtained under 35 °C differed significantly. Compared to the results reported by Li *et al.*,[49] where PHB degradation occurred at approximately 273 °C with a final degradation temperature of 280 °C, the PHB samples in this study exhibit slightly lower thermal stability, suggesting potential variations in polymer purity, molecular weight or crystallinity.

All samples have slightly lower thermal stability compared to a commercial poly[(3-hydroxybutyrate)-*co*-(3-hydroxyvalerate)] (PHBV) standard (92:8 molar ratio), which degraded at 287 °C (Fig. 5). This observation aligns with Li *et al.*,[49] who reported that the incorporation of 10 mol%–30 mol% of hydroxyvalerate in PHBV increased its thermal stability by 7 °C–12 °C. The lower thermal stability observed in this study suggests that the extracted polyhydroxyalkanoate may be a PHB homopolymer, which degrades more readily than its copolymer counterpart.

Additionally, all samples had residues below 10% except for the 35 °C biofilm sample, which retained more than 20% residue. The possible reasons for lower thermal stability observed in all PHB samples compared to commercial PHB could be due to differences in extraction methods. Pradhan *et al.*[50] demonstrated that PHB extracted using ultrasonic methods exhibited higher thermal stability (up to 289 °C) compared to solvent-extracted PHB, which degraded at 260 °C. The biofilm-grown PHB at 35 °C showed more prolonged mass loss and higher residue content, which is consistent with previous findings that biomass impurities and processing conditions affect thermal behavior.

The lower thermal stability and prolonged mass loss observed in the PHB sample obtained from biofilm biomass grown at 35 °C compared to other samples could be attributed to the presence of residual proteins or unreacted components. Hahn and Chang[48] noted that thermal degradation of cellular material alongside PHB can lead to overestimation of PHB content and altered thermal stability profiles. Similarly, Li *et al.*[49] found that PHB degradation occurs in a single weight-loss step, whereas PHBV exhibits multiple degradation events, supporting the observation that the molecular composition and processing history influence degradation behavior.

In summary, TGA revealed that PHB produced from suspended and biofilm growth at different temperatures exhibited distinct thermal degradation behaviors. The 30 °C suspended sample and 30 °C biofilm sample showed similar degradation patterns, whereas the 35 °C biofilm sample exhibited lower thermal stability and higher residual mass, possibly due to incomplete polymer purity and differences in crystallinity. These findings align with those of previous studies that indicate that microbial growth conditions and extraction techniques significantly influence the thermal properties of PHB.

Journal of Chemical Technology and Biotechnology published by John Wiley & Sons Ltd on behalf of Society of Chemical Industry (SCI).

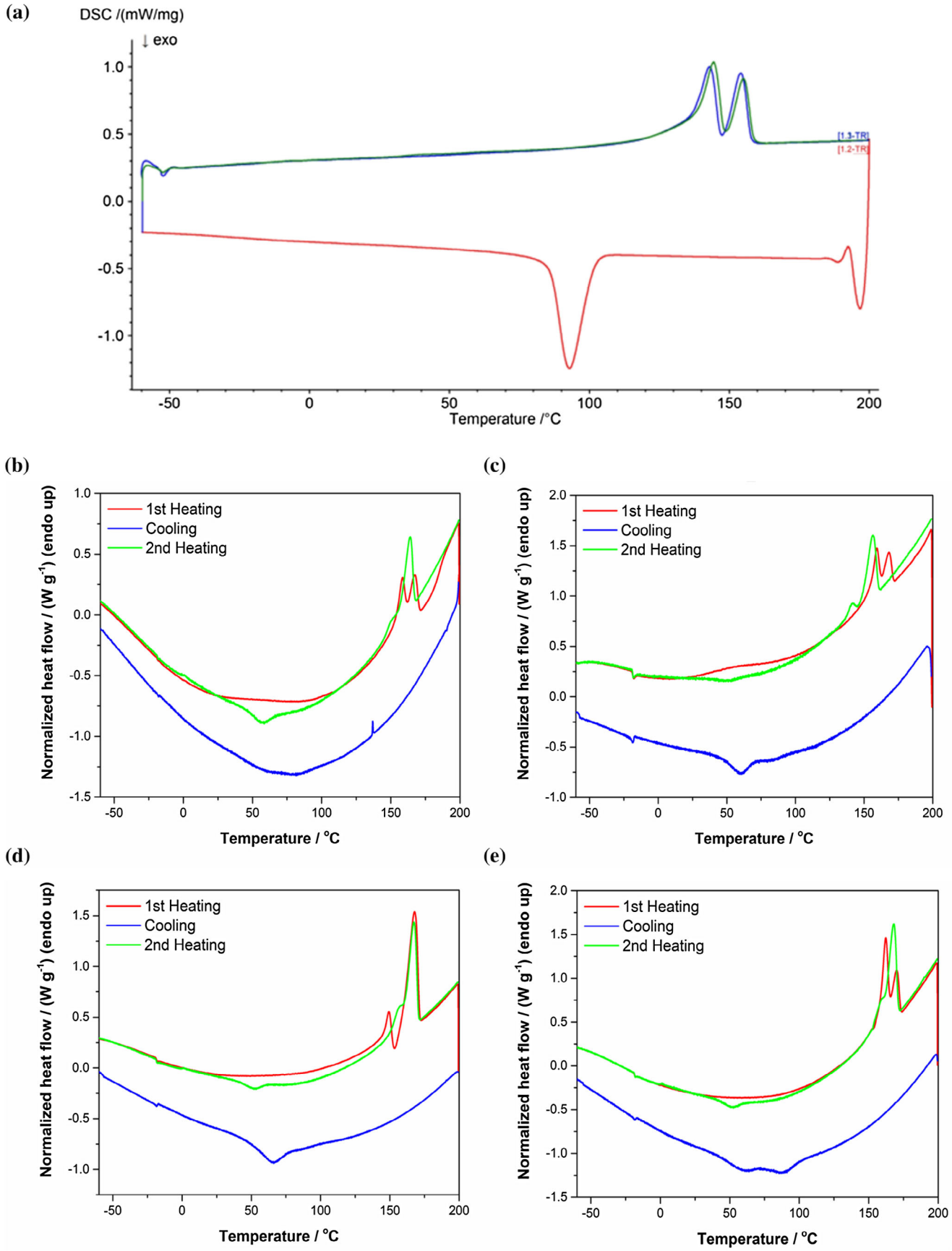

Figure 4. DSC of (a) standard PHB and of samples obtained from (b) suspended growth at 30 °C, (c) biofilm growth at 30 °C, (d) suspended growth at 35 °C and (e) biofilm growth at 35 °C.

Journal of Chemical Technology and Biotechnology published by John Wiley & Sons Ltd on behalf of Society of Chemical Industry (SCI).

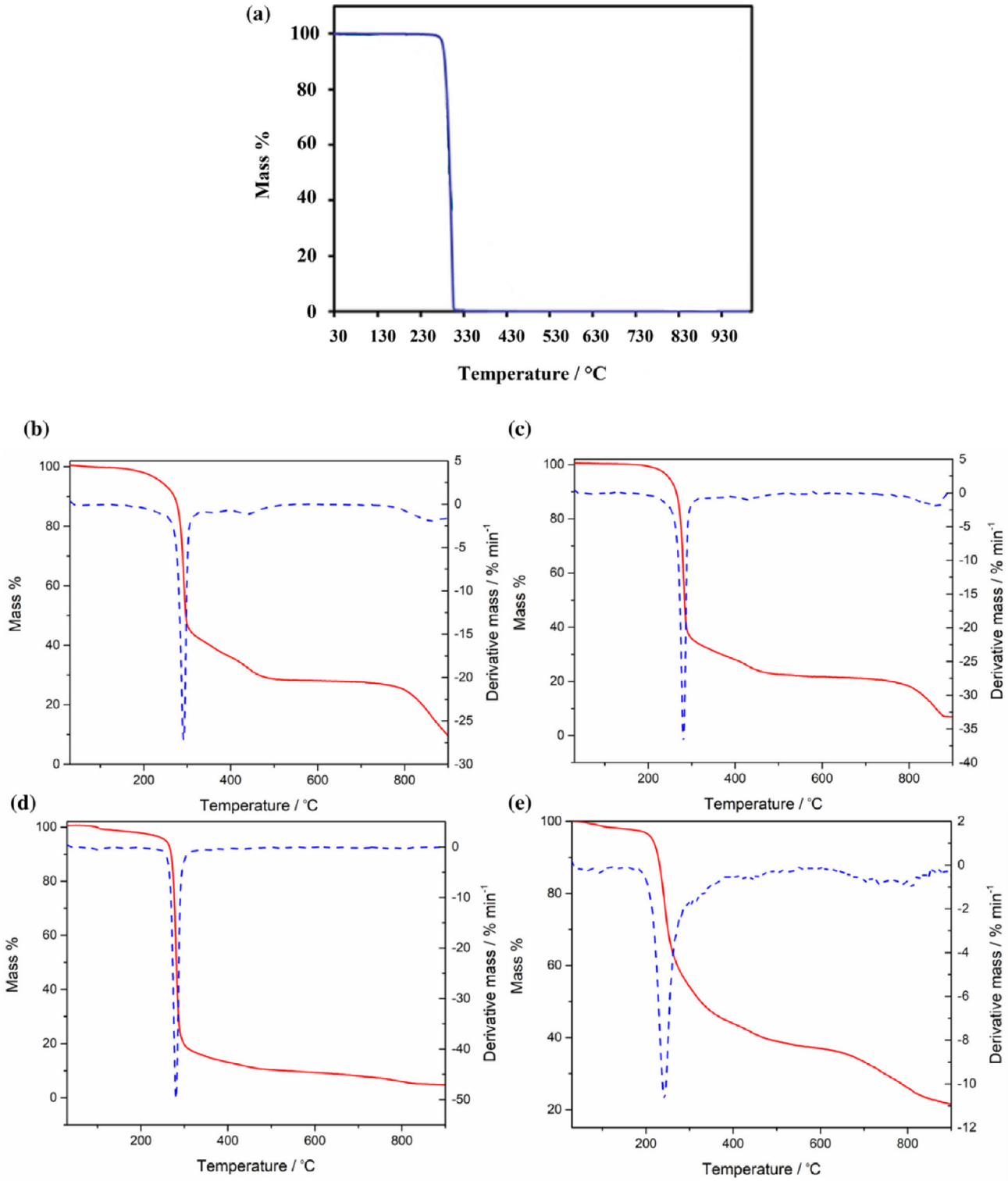

Figure 5. TGA of (a) standard PHB and of samples obtained from (b) suspended growth at 30 °C, (c) biofilm growth at 30 °C, (d) suspended growth at 35 °C and (e) biofilm growth at 35 °C.

FTIR spectroscopy

FTIR spectroscopy was used to analyze PHB samples obtained from suspended and biofilm growth at 30 °C and 35 °C. The FTIR spectra obtained from the samples showed similar absorption bands in the fingerprint region (500 cm^{-1}–4000 cm^{-1}), which is consistent with the presence of common functional groups such as C—H, C—O and C═O. The signal at 1728 cm^{-1} corresponds to the stretching of the carbonyl group (C═O), while the signal at 1280 cm^{-1} corresponds to the stretching of the ester group (C—O). The bands at 1380 cm^{-1}, 1228 cm^{-1} and 1180 cm^{-1} correspond to groups CH_3, CH_2 and C—O—C, respectively. The signal at 3250 cm^{-1} was only observed in the spectrum of the suspended

Journal of Chemical Technology and Biotechnology published by John Wiley & Sons Ltd on behalf of Society of Chemical Industry (SCI).

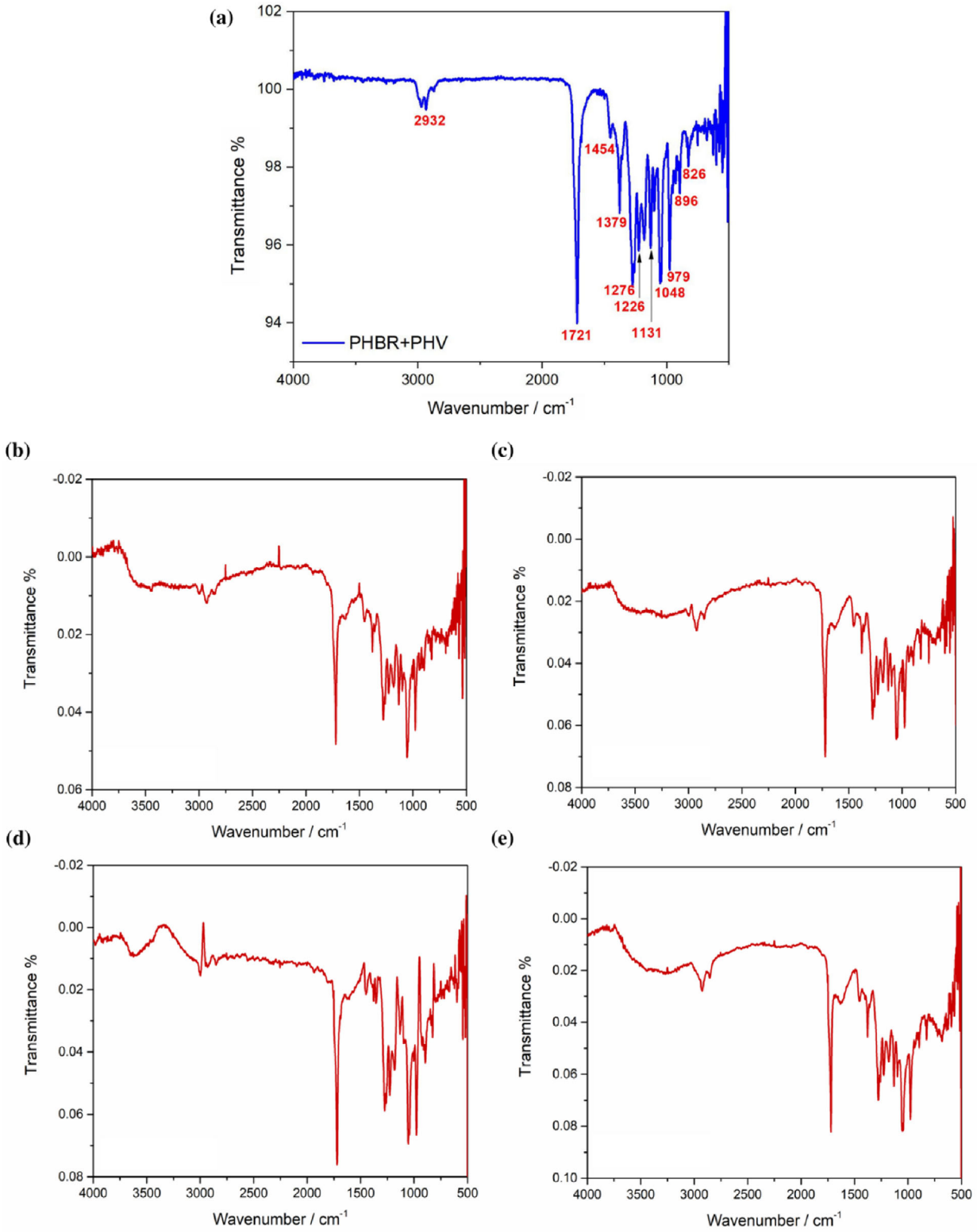

Figure 6. FTIR spectra of (a) standard PHB-PHBV and of samples obtained from (b) suspended growth at 30 °C, (c) biofilm growth at 30 °C, (d) suspended growth at 35 °C and (e) biofilm growth at 35 °C.

growth PHB sample obtained at 35 °C. It indicates the presence of hydroxyl (—OH) group. These signals are characteristic of PHB, confirming that the samples analyzed in this study are composed of this polymer (Fig. 6(a)–(c)).

Furthermore, the FTIR spectra obtained from PHB samples from suspended and biofilm growth at 35 °C (Fig. 6(d),(e)) showed similar signals to the samples obtained at 30 °C, indicating that the temperature change did not have a substantial impact on the

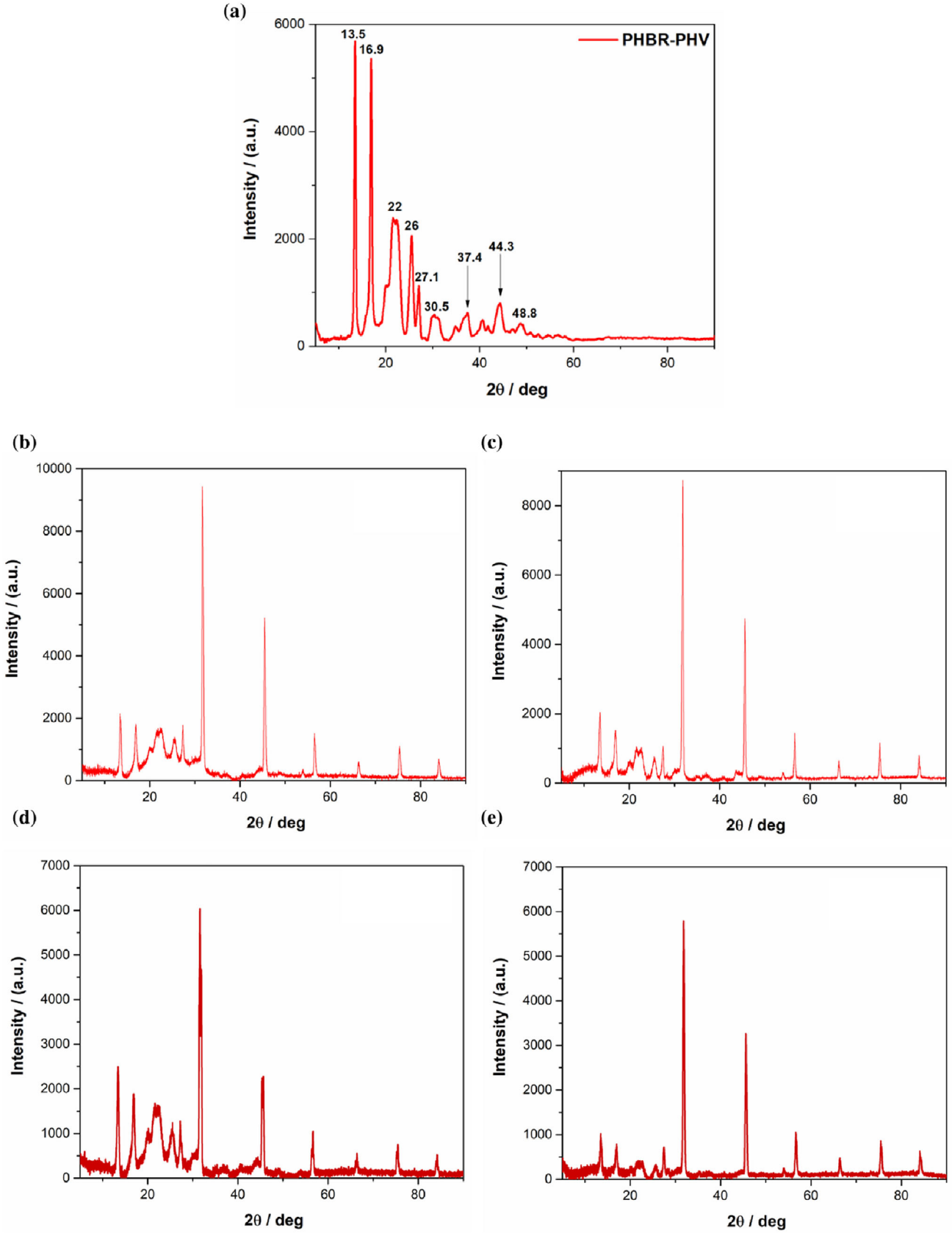

Figure 7. XRD patterns of (a) standard PHB and of samples obtained from (b) suspended growth at 30 °C, (c) biofilm growth at 30 °C, (d) suspended growth at 35 °C and (e) biofilm growth at 35 °C.

Journal of Chemical Technology and Biotechnology published by John Wiley & Sons Ltd on behalf of Society of Chemical Industry (SCI).

PHB composition. This aligns with the study by Deng *et al.*,[51] who analyzed PHB extracted from wastewater sludge and found that FTIR spectra remained consistent despite variations in microbial growth conditions. They reported a characteristic PHB peak range between 1728 cm^{-1} and 1754 cm^{-1}, which is in agreement with our findings. However, a discrepancy was observed when comparing our results with those of Hagagy *et al.*,[52] who reported a C═O stretching peak at 1628 cm^{-1} for PHB extracted from *Halolamina* species. This deviation in peak position may be attributed to differences in microbial sources, polymer purity or variations in polymer chain interactions for different extraction methods. Additionally, the presence of a strong absorption peak at 1728 cm^{-1} is consistent with findings from Ansari and Fatma,[53] who analyzed PHB extracted from cyanobacterial biomass. They reported similar FTIR spectra, with key peaks at 1720 cm^{-1}–1730 cm^{-1} and 1280 cm^{-1}, corroborating the functional group assignments in our study. However, their work indicated that additional peaks might arise due to variations in PHB purity and polymer chain length, which should be further investigated in our samples. Overall, the FTIR analysis confirmed the successful identification of PHB in all samples, with results aligning with previous literature while also revealing distinct spectral features such as the 3250 cm^{-1} hydroxyl peak, which warrants further investigation. The consistency in spectral characteristics across different temperature conditions further supports the robustness of PHB structural integrity under varied growth conditions.

XRD

XRD was used to analyze the crystal structure of the PHB samples obtained from suspended and biofilm growth at 30 °C and 35 °C. The XRD analysis revealed a prominent diffraction peak at 2θ of approximately 32°, corresponding to the (100) crystallographic plane of PHB, which is indicative of a high degree of crystallinity in the samples. This is consistent with previous studies, such as those by Phongtamrug and Tashiro,[54] who identified the same primary diffraction peak for PHB and confirmed its α-form crystalline structure under standard conditions. The presence of additional minor peaks at 45°, 58°, 68°, 70° and 84°, corresponding to the (200), (300), (411), (111) and (331) crystallographic planes, respectively, further supports the polycrystalline nature of the PHB samples (Fig. 7).

Interestingly, a distinct peak at 2θ of approximately 22° was observed exclusively in the suspended growth samples at both temperatures, corresponding to the (110) crystallographic plane, which was absent in the patterns of biofilm samples. This suggests differences in crystal orientation and molecular packing, likely influenced by the growth conditions rather than temperature alone. A similar phenomenon was reported by Etxabide *et al.*,[55] who found that PHB extracted from red grape pomace exhibited variations in crystallinity depending on the purification method, with more purified samples showing reduced crystallinity and altered peak intensity. This aligns with the current findings, as the differences in microbial growth conditions between biofilm and suspended cultures could have led to subtle alterations in the crystalline arrangement of PHB.

The degree of crystallinity in PHB can be affected by several factors, including synthesis conditions, processing methods and molecular weight distribution. The current results align with those of de Sousa Junior *et al.*,[56] who reported that PHB typically exhibits high crystallinity with characteristic peaks in the 2θ range 10°–35° and noted that crystallinity can be modulated by polymer interactions, blending or plasticizer addition. The absence of major structural changes between PHB grown at 30 °C and 35 °C suggests that temperature does not significantly influence PHB crystallinity, but, rather, growth conditions play a more dominant role. Similar findings were reported by Al-Jaber,[57] where polyhydroxyalkanoates extracted from PNSB exhibited comparable crystallinity patterns despite differences in substrate conditions, reinforcing that microbial metabolic pathways and polymer accumulation rates are more critical in defining the final crystal structure.

Overall, the XRD analysis confirmed that PHB produced under different microbial growth conditions maintains a highly crystalline structure, with key diffraction peaks corresponding to the α-form of PHB, as observed in previous studies. However, the minor differences between suspended and biofilm growth conditions, particularly the unique peak at $2\theta = 22°$ in the patterns of the suspended samples, suggest a variation in crystallographic arrangement, potentially due to differential polymer alignment or molecular stress during biosynthesis. These findings provide further insights into how microbial growth conditions influence PHB structural properties, a factor that should be considered in optimizing PHB production for various applications.

CONCLUSION

This study investigated the optimal temperature for FSW treatment, PNSB growth (both suspended and biofilm) and resource recovery using BPBRs operated at 30 °C, 35 °C and 45 °C. PNSB growth was not observed at 45 °C, confirming its metabolic limitations at high temperatures. The highest total biomass and suspended growth were achieved at 35 °C, whereas biofilm formation was more pronounced at 30 °C, likely due to reduced competition with suspended growth.

The findings highlight that biofilm growth supports higher PHB accumulation compared to suspended growth, emphasizing the role of growth mode in biopolymer synthesis. While PHB characteristics remained largely similar across conditions, slight differences in crystallinity were observed in suspended biomass. The lack of significant variation in PHB content between 30 °C and 35 °C suggests that temperature may have a limited effect on PHB biosynthesis under the tested conditions.

Furthermore, protein content remained stable across all temperature conditions, reinforcing the robustness of PNSB metabolic activity within the studied temperature range. These results highlight a key advantage of biofilm-based cultivation in terms of enhanced PHB production. Overall, this study demonstrates that PNSB biofilm systems can effectively contribute to wastewater treatment and sustainable PHB recovery, particularly in moderate-temperature environments.

AUTHOR CONTRIBUTIONS

Sultan Shaikh: Conceptualization, Data curation, Formal analysis, Visualization, Investigation, Writing - original draft, Writing - review and editing. **Soumia Gasmi:** PHB characterization. **Adriaan Stephanus Luyt:** Writing review and editing (PHB characterization), Funding acquisition. **Gordon McKay:** Writing - review and editing, Supervision. **Hamish Robert Mackey:** Funding acquisition, Project administration, Supervision, Resources, Writing - review and editing.

ACKNOWLEDGEMENTS

The authors extend their appreciation to the Qatar Shell Research and Technology Centre for its invaluable technical assistance and

Journal of Chemical Technology and Biotechnology published by John Wiley & Sons Ltd on behalf of Society of Chemical Industry (SCI).

to the laboratory management team at the Hamad Bin Khalifa University–College of Science and Engineering for their logistical support.

FUNDING INFORMATION

This research received funding from the Qatar National Research Fund under the National Priorities Research Program (grant number NPRP11-S-0110-180245). The Qatar National Library provided the open access funding.

DATA AVAILABILITY STATEMENT

Data will be made available on request.

CONFLICT OF INTEREST

The authors state that there are no known financial conflicts of interest or personal connections that might seem to affect the findings presented in this document.

SUPPORTING INFORMATION

Supporting information may be found in the online version of this article.

REFERENCES

1 Froment T, Zero liquid discharge at the world's largest gas-to-liquid plant (2016).
2 US Energy Information Administration, Global gas-to-liquids growth is dominated by two projects in South Africa and Uzbekistan, in *Today in Energy*. Energy Information Administration, Washington, DC, pp. 1–2 (2017).
3 Zacharia R, El-Naas MH and Al-Marri MJ, Photocatalytic oxidation of non-acid oxygenated hydrocarbons, in *Water Manag*. CRC Press, Boca Raton, Florida, pp. 287–302 (2019).
4 Guerra SR, Oulego P, Rodríguez E, Singh DN and Rodríguez-Chueca J, Towards the implementation of circular economy in the wastewater sector: challenges and opportunities. *Water (Basel)* **12**:1431 (2020). https://doi.org/10.3390/w12051431.
5 Puyol D, Batstone DJ, Hülsen T, Astals S, Peces M and Krömer JO, Resource recovery from wastewater by biological technologies: opportunities, challenges, and prospects. *Front Microbiol* **7**:2106 (2017). https://doi.org/10.3389/FMICB.2016.02106.
6 Yu Q, Pei X, Wei Y, Naveed S, Wang S, Chang M *et al*., The roles of bacteria in resource recovery, wastewater treatment and carbon fixation by microalgae-bacteria consortia: a critical review. *Algal Res* **69**:102938 (2023). https://doi.org/10.1016/j.algal.2022.102938.
7 Alloul A, Wille M, Lucenti P, Bossier P, van Stappen G and Vlaeminck SE, Purple bacteria as added-value protein ingredient in shrimp feed: *Penaeus vannamei* growth performance, and tolerance against vibrio and ammonia stress. *Aquaculture* **530**:735788 (2021). https://doi.org/10.1016/j.aquaculture.2020.735788.
8 Wada OZ, Vincent AS and Mackey HR, Single-cell protein production from purple non-sulphur bacteria-based wastewater treatment. *Rev Environ Sci Bio/Technology* **214**:931–956 (2022). https://doi.org/10.1007/S11157-022-09635-Y.
9 Shaikh S, Rashid N, Onwusogh U, McKay G and Mackey HR, Effect of nutrients deficiency on biofilm formation and single cell protein production with a purple non-sulphur bacteria enriched culture. *Biofilms* **5**:100098 (2023). https://doi.org/10.1016/J.BIOFLM.2022.100098.
10 Charlton PJ, Thermotolerant purple nonsulfur bacteria from New Zealand geothermal areas (2002).
11 Hisada T, Okamura K and Hiraishi A, Isolation and characterization of phototrophic purple nonsulfur bacteria from *Chloroflexus* and cyanobacterial mats in hot springs. *Microbes Environ* **22**:405–411 (2007). https://doi.org/10.1264/JSME2.22.405.
12 Kaftan D, Bína D and Koblížek M, Temperature dependence of photosynthetic reaction centre activity in *Rhodospirillum rubrum*. *Photosynth Res* **142**:181–193 (2019). https://doi.org/10.1007/S11120-019-00652-7.
13 Kaiser I and Oelze J, Temperature dependence of membrane-bound enzymes of the energy metabolism in *Rhodospirillum rubrum* and *Rhodopseudomonas sphaeroides*. *Arch Microbiol* **126**:195–200 (1980). https://doi.org/10.1007/BF00511227.
14 Lee YR, Nur Fitriana H, Lee SY, Kim MS, Moon M, Lee WH *et al*., Molecular profiling and optimization studies for growth and PHB production conditions in *Rhodobacter sphaeroides*. *Energies* **13**:6471 (2020). https://doi.org/10.3390/EN13236471.
15 Lo KJ, Lee SK and Liu C, Development of a low-cost culture medium for the rapid production of plant growth-promoting *Rhodopseudomonas palustris* strain PS3. *PLoS One* **15**:e0236739 (2020). https://doi.org/10.1371/JOURNAL.PONE.0236739.
16 Hülsen T, Stegman S, Batstone DJ and Capson-Tojo G, Naturally illuminated photobioreactors for resource recovery from piggery and chicken-processing wastewaters utilising purple phototrophic bacteria. *Water Res* **214**:118194 (2022). https://doi.org/10.1016/j.watres.2022.118194.
17 Shaikh S, Rashid N, McKay G, Liberski AR and Mackey HR, Nitrogen influence on suspended vs biofilm growth and resource recovery potential of purple non-sulfur bacteria treating fuel synthesis wastewater. *Biochem Eng J* **190**:1–10 (2023). https://doi.org/10.1016/j.bej.2022.108754.
18 APHA, *Standard Methods for the Examination of Water and Wastewater*, Vol. **51**. American Public Health Association, Washington, DC, p. 940 (2012).
19 Hach, Oxygen Demand, Chemical, in *USEPA Reactor Digestion Method. Hach Method. 8000*. Hach Company, Loveland, Colorado, USA, pp. 1–6 (2019).
20 Sali S and Mackey HR, The application of purple non-sulfur bacteria for microbial mixed culture polyhydroxyalkanoates production. *Rev Environ Sci Biotechnol* **20**:959–983 (2021). https://doi.org/10.1007/s11157-021-09597-7.
21 Rabilloud G, 9-heat-resistant adhesives a2-ebnesajjad, sina, in *Handbook of Adhesives and Surface Preparation*. William Andrew, Norwich, New York, USA, pp. 137–183 (2011).
22 Lowry O, Schagger H, Cramer WA and Vonjagow G, Protein measurement with the Folin phenol reagent. *Anal Biochem* **217**:220–230 (1994).
23 Perović MN, Jugović ZDK and Antov MG, Improved recovery of protein from soy grit by enzyme-assisted alkaline extraction. *J Food Eng* **276**:1–9 (2020). https://doi.org/10.1016/j.jfoodeng.2019.109894.
24 Bligh E and Dyer WJ, A rapid method of total lipid extraction and purification. *Can J Biochem Physiol* **37**:911–917 (1959). https://doi.org/10.1139/o59-099.
25 Morris DL, Quantitative determination of carbohydrates with Dreywood's anthrone reagent. *Science* **107**:254–255 (1948). https://doi.org/10.1126/science.107.2775.254.
26 Chumpol S, Kantachote D, Nitoda T and Kanzaki H, Administration of purple nonsulfur bacteria as single cell protein by mixing with shrimp feed to enhance growth, immune response and survival in white shrimp (*Litopenaeus vannamei*) cultivation. *Aquaculture* **489**:85–95 (2018). https://doi.org/10.1016/j.aquaculture.2018.02.009.
27 Brankarl L, Yoneyama H, Iwata T, Kim JS, Okuda SI, Kampee T *et al*., Growth of non-sulfur purple photosynthetic bacteria under high temperature. *Bull Jpn Soc Microb Ecol* **2**:13–19 (1987). https://doi.org/10.1264/microbes1986.2.13.
28 Sepúlveda-Muñoz CA, Torres-Franco AF, de Godos I and Muñoz R, Exploring the metabolic capabilities of purple phototrophic bacteria during piggery wastewater treatment. *J Water Process Eng* **50**:103317 (2022). https://doi.org/10.1016/j.jwpe.2022.103317.
29 Segura PC, De Meur Q, Tanghe A, Cabecas Segura P, Onderwater R, Dewasme L *et al*., Effects of mixing volatile fatty acids as carbon sources on *Rhodospirillum rubrum* carbon metabolism and redox balance mechanisms. *Microorganisms* **9**:1996 (2021). https://doi.org/10.3390/microorganisms9091996.
30 Hiraishi A, Nagao N, Yonekawa C, Umekage S, Kikuchi Y, Eki T *et al*., Distribution of phototrophic purple nonsulfur bacteria in massive blooms in coastal and wastewater ditch environments. *Microorganisms* **8**:1–19 (2020). https://doi.org/10.3390/microorganisms8020150.
31 Vasiliadou IA, Berná A, Manchon C, Melero JA, Martinez F, Esteve-Nuñez A *et al*., Biological and bioelectrochemical systems

Journal of Chemical Technology and Biotechnology published by John Wiley & Sons Ltd on behalf of Society of Chemical Industry (SCI).

for hydrogen production and carbon fixation using purple phototrophic bacteria. *Front Energy Res* **6**:1–12 (2018). https://doi.org/10.3389/fenrg.2018.00107.
32 Capson-Tojo G, Batstone DJ, Grassino M, Vlaeminck SE, Puyol D, Verstraete W *et al*., Purple phototrophic bacteria for resource recovery: challenges and opportunities. *Biotechnol Adv* **43**:107567 (2020). https://doi.org/10.1016/j.biotechadv.2020.107567.
33 Carlozzi P, Di Lorenzo T, Ghanotakis DF and Touloupakis E, Effects of pH, temperature and salinity on P3HB synthesis culturing the marine *Rhodovulum sulfidophilum* DSM-1374. *Appl Microbiol Biotechnol* **104**:2007–2015 (2020). https://doi.org/10.1007/s00253-020-10352-1.
34 Hülsen T, Barry EM, Lu Y, Puyol D, Keller J and Batstone DJ, Domestic wastewater treatment with purple phototrophic bacteria using a novel continuous photo anaerobic membrane bioreactor. *Water Res* **100**:486–495 (2016). https://doi.org/10.1016/j.watres.2016.04.061.
35 Hülsen T, Batstone DJ and Keller J, Phototrophic bacteria for nutrient recovery from domestic wastewater. *Water Res* **50**:18–26 (2014). https://doi.org/10.1016/j.watres.2013.10.051.
36 Inglesby AE, Beatty DA and Fisher AC, *Rhodopseudomonas palustris* purple bacteria fed *Arthrospira maxima* cyanobacteria: demonstration of application in microbial fuel cells. *RSC Adv* **2**:4829–4838 (2012). https://doi.org/10.1039/c2ra20264f.
37 Fradinho JC, Reis MAM and Oehmen A, Beyond feast and famine: selecting a PHA accumulating photosynthetic mixed culture in a permanent feast regime. *Water Res* **105**:421–428 (2016). https://doi.org/10.1016/j.watres.2016.09.022.
38 Padovani G, Carlozzi P, Seggiani M, Cinelli P, Vitolo S and Lazzeri A, PHB-rich biomass and BioH2 production by means of photosynthetic microorganisms. *Chem Eng Trans* **49**:55–60 (2016). https://doi.org/10.3303/CET1649010.
39 Asad-ur-Rehman AU, Alia Aslam AA, Rushda Masood RM, Aftab MN, Rabia Ajmal RA and Ikram-ul-Haq IU, Production and characterization of a thermostable bioplastic (poly-s-hydroxybutyrate) from *Bacillus cereus* NRRL-b-3711. *Pak J Bot* **48**:349–356 (2016).
40 Mansilla MC, Cybulski LE, Albanesi D and De Mendoza D, Control of membrane lipid fluidity by molecular thermosensors. *J Bacteriol* **186**:6681–6688 (2004). https://doi.org/10.1128/JB.186.20.6681-6688.2004.
41 Tedesco MA and Duerr EO, Light, temperature and nitrogen starvation effects on the total lipid and fatty acid content and composition of Spirulina platensis UTEX 1928. *J Appl Phycol* **1**:201–209 (1989). https://doi.org/10.1007/BF00003646.
42 de Carvalho Silvello MA, Severo Gonçalves I, Patrícia Held Azambuja S, de Carvalho Silvello MA, Silva Costa S, Garcia Pereira Silva P *et al*., Microalgae-based carbohydrates: a green innovative source of bioenergy. *Bioresour Technol* **344**:126304 (2022). https://doi.org/10.1016/j.biortech.2021.126304.
43 Hülsen T, Sander EM, Jensen PD and Batstone DJ, Application of purple phototrophic bacteria in a biofilm photobioreactor for single cell protein production: biofilm vs suspended growth. *Water Res* **181**:1–10 (2020). https://doi.org/10.1016/j.watres.2020.115909.
44 Kuo FS, Chien YH and Chen CJ, Effects of light sources on growth and carotenoid content of photosynthetic bacteria *Rhodopseudomonas palustris*. *Bioresour Technol* **113**:315–318 (2012). https://doi.org/10.1016/j.biortech.2012.01.087.
45 Meng F, Yang A, Wang H, Zhang G, Li X, Zhang Y *et al*., One-step treatment and resource recovery of high-concentration non-toxic organic wastewater by photosynthetic bacteria. *Bioresour Technol* **251**:121–127 (2018). https://doi.org/10.1016/j.biortech.2017.12.002.
46 Zhou Q, Zhang P and Zhang G, Biomass and carotenoid production in photosynthetic bacteria wastewater treatment: effects of light intensity. *Bioresour Technol* **171**:330–335 (2014). https://doi.org/10.1016/j.biortech.2014.08.088.
47 Mohd Zahari MAK, Ariffin H, Mokhtar MN, Salihon J, Shirai Y and Hassan MA, Factors affecting poly(3-hydroxybutyrate) production from oil palm frond juice by *Cupriavidus necator* (CCUG52238 T). *J Biomed Biotechnol* **2012**:1–8 (2012). https://doi.org/10.1155/2012/125865.
48 Hahn SK and Chang YK, A themogravimetric analysis for poly(3-hydroxybutyrate) quantification. *Biotechnol Tech* **9**:873–878 (1995). https://doi.org/10.1007/BF00158539.
49 Li SD, Yu PH and Cheung MK, Thermogravimetric analysis of poly(3-hydroxybutyrate) and poly(3-hydroxybutyrate-co-3-hydroxyvalerate). *J Appl Polym Sci* **80**:2237–2244 (2001). https://doi.org/10.1002/app.1327.
50 Pradhan S, Dikshit PK and Moholkar VS, Production, ultrasonic extraction, and characterization of poly(3-hydroxybutyrate) (PHB) using *Bacillus megaterium* and *Cupriavidus necator*. *Polym Adv Technol* **29**:2392–2400 (2018). https://doi.org/10.1002/pat.4351.
51 Deng B, Rao L and Rodriguez-Freire L, Evaluation and optimization of FTIR spectroscopy to quantify PHA production by municipal wastewater sludge. *Spectrochim Acta A* **312**:124012 (2024). https://doi.org/10.1016/j.saa.2024.124012.
52 Hagagy N, Saddiq AA, Tag HM, Selim S, AbdElgawad H and Martínez-Espinosa RM, Characterization of polyhydroxybutyrate, PHB, synthesized by newly isolated haloarchaea *Halolamina* spp. *Molecules* **27**:7366 (2022). https://doi.org/10.3390/molecules27217366.
53 Ansari S and Fatma T, Cyanobacterial polyhydroxybutyrate (PHB): screening, optimization and characterization. *PLoS One* **11**:e0158168 (2016). https://doi.org/10.1371/journal.pone.0158168.
54 Phongtamrug S and Tashiro K, X-ray crystal structure analysis of poly(3-hydroxybutyrate) β-form and the proposition of a mechanism of the stress-induced α-to-β phase transition. *Macromolecules* **52**:2995–3009 (2019). https://doi.org/10.1021/acs.macromol.9b00225.
55 Etxabide A, Kilmartin PA, Guerrero P, de la Caba K, Hooks DO, West M *et al*., Polyhydroxybutyrate (PHB) produced from red grape pomace: effect of purification processes on structural, thermal and antioxidant properties. *Int J Biol Macromol* **217**:449–456 (2022). https://doi.org/10.1016/j.ijbiomac.2022.07.072.
56 de Sousa Junior RR, dos Santos CAS, Ito NM, Suqueira AN, Lackner M and dos Santos DJ, PHB processability and property improvement with linear-chain polyester oligomers used as plasticizers. *Polymers (Basel)* **14**:4197 (2022). https://doi.org/10.3390/polym14194197.
57 Al-Jaber NKJ, Extraction and characterization of polyhydroxyalkanoates from purple non-sulfur bacteria treating fuel synthesis process water. Master's thesis, Hamad Bin Khalifa University, Qatar (2021).

Journal of Chemical Technology and Biotechnology published by John Wiley & Sons Ltd on behalf of Society of Chemical Industry (SCI).